

Research



Cite this article: Mesarovic SD, Forest S, Jaric JP. 2015 Size-dependent energy in crystal plasticity and continuum dislocation models. *Proc. R. Soc. A* **471**: 20140868. <http://dx.doi.org/10.1098/rspa.2014.0868>

Received: 7 November 2014

Accepted: 20 January 2015

Subject Areas:

mechanical engineering, materials science, mechanics

Keywords:

coarsening, mesoscale models, geometrically necessary dislocations, crystal symmetries, material length scales

Author for correspondence:

Sinisa Dj. Mesarovic

e-mail: mesarovic@mme.wsu.edu

Size-dependent energy in crystal plasticity and continuum dislocation models

Sinisa Dj. Mesarovic¹, Samuel Forest² and

Jovo P. Jaric³

¹School of Mechanical and Materials Engineering, Washington State University, Pullman, WA 99164, USA

²Centre des Matériaux, Mines ParisTech/CNRS UMR 7633, BP 87, 91003 Evry Cedex, France

³Faculty of Mathematics, University of Belgrade, Jagiceva 5, 11000 Belgrade, Serbia

 SDM, 0000-0002-0117-426X; SF, 0000-0002-8869-3942

In the light of recent progress in coarsening the discrete dislocation mechanics, we consider two questions relevant for the development of a mesoscale, size-dependent plasticity: (i) can the phenomenological expression for size-dependent energy, as quadratic form of Nye's dislocation density tensor, be justified from the point of view of dislocation mechanics and under what conditions? (ii) how can physical or phenomenological expressions for size-dependent energy be computed from dislocation mechanics in the general case of elastically anisotropic crystal? The analysis based on material and slip system symmetries implies the negative answer to the first question. However, the coarsening method developed in response to the second question, and based on the physical interpretation of the size-dependent energy as the coarsening error in dislocation interaction energy, introduces additional symmetries. The result is that the equivalence between the phenomenological and the physical expressions is possible, but only if the multiplicity of characteristic lengths associated with different slip systems, is sacrificed. Finally, we discuss the consequences of the assumption that a single length scale governs the plasticity of a crystal, and note that the plastic dissipation at interfaces has a strong dependence on the length scale embedded in the energy expression.

1. Introduction

Following numerous observations of size effects in plasticity of metals and Ashby's [1] analysis of geometrically necessary and statistically stored dislocations (GND and SSD), equally numerous phenomenological theories have appeared in the past two decades, of which we take Gurtin's [2] crystal plasticity as the representative one. In addition to the theories directly concerned with plasticity of crystals, some generalized continua inspired by early works in polar or micromorphic continua, [3,4] such as the microcurvature theory [5,6], include the size-dependent crystal plasticity, as a special case. Finally, the special class of dynamical theories, statistical continuum dislocation dynamics (SCDD), is under development [7–9]. This formulation includes the dynamic evolution of dislocations represented as continuum density fields.

The size-dependent portion of internal energy is typically a function of Nye's [10] or Kröner's [11] dislocation density tensor, or its finite deformation generalization [12,13]. Because this portion of energy has its roots in elastic interactions of dislocations, the quadratic form leading to a linear constitutive law is appropriate

$$\frac{1}{2} \mathbf{A} : \mathbf{M} : \mathbf{A} = \frac{1}{2} A_{ji} M_{ijkl} A_{lk}. \quad (1.1)$$

The components of Nye's [10] dislocation density tensor \mathbf{A} are defined as the components of the net Burgers vector in a representative volume element (RVE) associated with dislocation line directions. If the dislocation segment type¹ $I (I = 1, \dots, N_T)$ is defined by its Burgers vector \mathbf{b}^I and its line direction ξ^I , and each type is characterized by its density (line length per unit volume) ρ^I , then the Nye's tensor is given as the sum of dyads

$$\mathbf{A} = \sum_{I=1}^{N_T} \rho^I \mathbf{b}^I \xi^I = \sum_{I=1}^{N_T} (\rho b)^I \mathbf{s}^I \xi^I; \quad b = |\mathbf{b}|; \quad \mathbf{s} = \frac{\mathbf{b}}{b}. \quad (1.2)$$

The densities $(\rho b)^I$ are, in general, not uniquely defined from the Nye's tensor [14].

Dimensionally, the components of the rank-4 constitutive tensor \mathbf{M} are products of an elastic modulus and the square of a characteristic length responsible for size-dependence. The phenomenological theories, based on the existence of representation (1.1), also rely on the ability to (in principle) fit the components of \mathbf{M} to experimental data.

Advances in experimental methods, in particular EBSD, have allowed researchers to measure lattice curvatures at very small scales [15–17] and compute the Nye's tensor from the lattice curvature tensor. Naturally, the question of deconstruction of Nye's tensor into dislocation densities arises. Because purely kinematic deconstruction is not unique, additional conditions, typically minimization of some norms of dislocation densities, are used to obtain a unique deconstruction². The quadratic form (1.1) is one such norm.

In this paper, we compare the phenomenological size-dependent energy (1.1) to analogous energy representations in recently developed physical theories [18,19]. Because the later are developed on the basis of dislocation mechanics, they serve as the benchmark for the phenomenological expression (1.1). The main questions addressed in this paper are

1. Can the phenomenological size-dependent energy (1.1) represent the physical expressions, and under which conditions?
2. How can the size-dependent energy be computed on the basis of dislocation mechanics?

The paper is organized as follows.

In §2, we discuss the material symmetries that must be satisfied by the tensor \mathbf{M} (1.1). In §3, the summary of physical theories, based on dislocation mechanics and statistics of dislocations, is

¹To simplify the discussion, we consider, without loss of generality, straight segment in a RVE.

²The resulting pseudo-inversion to (1.2) is nonlinear and involves a particularly vexing type of nonlinearity with Boolean queries on linear combinations of Nye's components. See Kysar *et al.* [17] for an illustrative example.

given. In §4, we discuss the mathematical equivalence conditions between the phenomenological and physical theories, whereas in §5, we consider additional symmetries arising from the geometry of slip systems. Section 6 is devoted to the method of coarsening dislocation mechanics to compute the size-dependent energy. We conclude the paper in §7, with the discussion on the importance of multiple length scales.

2. Material symmetries

The tensor \mathbf{M} is subjected to the major symmetry restriction imposed by the quadratic form³ (1.1):

$$M_{ijkl} = M_{klij}, \quad (2.1)$$

so that it can have no more than 45 independent components.

The Nye's tensor, as defined in (1.2), is a dyadic product of vectors which are transformed by an orthogonal transformation in a standard way. Let \mathbf{Q} be an orthogonal transformation. Then

$$\left. \begin{aligned} \mathbf{A}' &= \langle \mathbf{Q} \rangle^2 * \mathbf{A} = A_{ij}(\mathbf{Q} \cdot \mathbf{e}_i)(\mathbf{Q} \cdot \mathbf{e}_j); \\ \mathbf{M}' &= \langle \mathbf{Q} \rangle^4 * \mathbf{M} = M_{ijkl}(\mathbf{Q} \cdot \mathbf{e}_i)(\mathbf{Q} \cdot \mathbf{e}_j)(\mathbf{Q} \cdot \mathbf{e}_k)(\mathbf{Q} \cdot \mathbf{e}_l), \end{aligned} \right\} \quad (2.2)$$

where asterisk is the Rayleigh product [20] and $\langle \mathbf{Q} \rangle^4$ is the fourth Kronecker power of \mathbf{Q} [21]. The energy (1.1) is a scalar invariant. We note, for later use, that transformations (2.2) are linear. Further, if \mathbf{Q} is in the symmetry group of the material, \mathbf{M} is invariant under the transformation

$$\langle \mathbf{Q} \rangle^4 * \mathbf{M} = \mathbf{M}. \quad (2.3)$$

Symmetries of tensors analogous to \mathbf{M} have been analysed in the context of polar continua, where non-symmetric tensors, such as \mathbf{A} , enter quadratic forms describing energy densities [21–23]. For materials with isotropic, cubic and hexagonal symmetries, there are three, four and eight independent constants, respectively. Define the *canonical* orthonormal crystal base triad $\mathbf{e}_i (i = 1, 2, 3)$. For cubic crystals, the canonical base is aligned with the edges of the cubic unit cell. Further, let $\mathbf{p}_i (i = 1, 2, 3)$ be an arbitrary orthonormal base. In the *isotropic* case, the canonical system plays no special role, so that the tensor \mathbf{M} and the elastic stiffness tensor \mathbf{C} can be written as

$$\left. \begin{aligned} \mathbf{M} &= M_1 \mathbf{p}_i \mathbf{p}_i \mathbf{p}_j \mathbf{p}_j + M_2 \mathbf{p}_i \mathbf{p}_j \mathbf{p}_i \mathbf{p}_j + M_3 \mathbf{p}_i \mathbf{p}_j \mathbf{p}_i \mathbf{p}_j; \\ \mathbf{C} &= C_1 \mathbf{p}_i \mathbf{p}_i \mathbf{p}_j \mathbf{p}_j + C_2 (\mathbf{p}_i \mathbf{p}_j \mathbf{p}_j \mathbf{p}_i + \mathbf{p}_i \mathbf{p}_j \mathbf{p}_i \mathbf{p}_j). \end{aligned} \right\} \quad (2.4)$$

For material with *cubic* symmetries

$$\left. \begin{aligned} \mathbf{M} &= M_0 \sum_{\alpha=1}^3 \mathbf{e}_\alpha \mathbf{e}_\alpha \mathbf{e}_\alpha \mathbf{e}_\alpha + M_1 \mathbf{p}_i \mathbf{p}_i \mathbf{p}_j \mathbf{p}_j + M_2 \mathbf{p}_i \mathbf{p}_j \mathbf{p}_i \mathbf{p}_j + M_3 \mathbf{p}_i \mathbf{p}_j \mathbf{p}_i \mathbf{p}_j; \\ \mathbf{C} &= C_0 \sum_{\alpha=1}^3 \mathbf{e}_\alpha \mathbf{e}_\alpha \mathbf{e}_\alpha \mathbf{e}_\alpha + C_1 \mathbf{p}_i \mathbf{p}_i \mathbf{p}_j \mathbf{p}_j + C_2 (\mathbf{p}_i \mathbf{p}_j \mathbf{p}_j \mathbf{p}_i + \mathbf{p}_i \mathbf{p}_j \mathbf{p}_i \mathbf{p}_j). \end{aligned} \right\} \quad (2.5)$$

The usual summation over repeated indices applies, unless Greek alphabet is used.

3. Physical theories and length scales

We are aware of only two attempts to derive the size-dependent energy from the mechanics of discrete dislocations. Motivated by needs of SCDD needs, Groma [24] and Groma *et al.* [18] consider a two-dimensional random field of dislocations and apply the analysis based on the self-consistent method ('Debye screening'). Not surprisingly, the analysis of a random field yields a single characteristic length—the average spacing of dislocations. Noting that such characteristic

³The skew portion ($M_{ijkl} - M_{klij}$) does not contribute to (1.1). Alternatively, one may invoke the elastic reciprocity theorem.

length evolves on a slower timescale than plastic deformation, the results can be linearized. Upon generalizing to three-dimensional, the size-dependent portion of the total energy will take the form

$$\frac{1}{2} \{\rho b\}^T [K] \{\rho b\} = \frac{1}{2} \sum_{I=1}^{N_T} \sum_{J=1}^{N_T} (\rho b)^I K^{IJ} (\rho b)^J. \quad (3.1)$$

The quadratic form in (3.1) requires the symmetry

$$K^{IJ} = K^{JI}. \quad (3.2)$$

Dimensionally, K^{IJ} are products of elastic moduli and the square of the characteristic length. The Burgers vector, \mathbf{b}^I in (1.2), is defined relative to line direction ξ^I , so that the pairs (\mathbf{b}, ξ) and $(-\mathbf{b}, -\xi)$ count as a single type. This ambiguity is resolved if dislocation densities are defined from slip gradients [25], as follows.

The standard definition of the slip system α ($\alpha = 1, \dots, N_S$) includes the slip plane normal \mathbf{m}^α and the slip direction \mathbf{s}^α . Both are unit vectors and the latter is parallel to the Burgers vector. The triad $(\mathbf{s}^\alpha, \mathbf{m}^\alpha, \mathbf{t}^\alpha = \mathbf{s}^\alpha \times \mathbf{m}^\alpha)$ forms the local orthonormal basis for the slip system. The slip field $\gamma^\alpha(\mathbf{x})$ is associated with each slip system. The in-plane components of its gradient define the *partial densities* of edge (\perp) and screw (\odot) dislocations, i.e. the densities *resulting only from slip evolution on that slip system*

$$g_{\perp}^\alpha = \mathbf{s}^\alpha \cdot \nabla \gamma^\alpha; \quad g_{\odot}^\alpha = \mathbf{t}^\alpha \cdot \nabla \gamma^\alpha; \quad \mathbf{g}^\alpha = g_{\odot}^\alpha \mathbf{t}^\alpha + g_{\perp}^\alpha \mathbf{s}^\alpha. \quad (3.3)$$

Nye's dislocation density tensor \mathbf{A} can be defined from the partial densities:

$$\mathbf{A} = - \sum_{\alpha=1}^{N_S} \mathbf{s}^\alpha (\mathbf{m}^\alpha \times \mathbf{g}^\alpha) = \sum_{\alpha=1}^{N_S} (-g_{\odot}^\alpha \mathbf{s}^\alpha \mathbf{s}^\alpha + g_{\perp}^\alpha \mathbf{s}^\alpha \mathbf{t}^\alpha). \quad (3.4)$$

As in the case of definition (1.2), the inverse mapping is not unique, i.e. the partial densities are not uniquely defined from the Nye's tensor.

The list of partial densities $\{g\}$ has $2N_S$ elements, and the list of densities $\{\rho\}$ has N_T elements. Because some slip systems share slip direction, and stationary screw dislocations are oblivious to the slip plane: $N_T \leq 2N_S$. For example, in *fcc* crystals, $2N_S = 24$ and $N_T = 18$. The *kinematic redundancy* in description (3.3) is resolved by simply adding the components g_{\odot}^α of the two slip systems (α and α') which share the slip direction

$$(\rho b)^I \xi^I = g_{\odot}^\alpha \mathbf{s}^\alpha + g_{\odot}^{\alpha'} \mathbf{s}^{\alpha'}. \quad (3.5)$$

The compliance with any local definition of Burgers vector [26] is accomplished by requiring that the dislocation line direction, ξ , always follows one rule with respect to \mathbf{m}^α : either the right-hand rule or the left-hand rule [25].

We note that both sets of dislocation densities $\{\rho\}$ and $\{g\}$ are *crystallographic densities*, i.e. defined with respect to crystallographic slip systems. In general, stationary dislocations may be formed as the result of relaxation and need not be constrained with slip system geometry [14].

In contrast to Groma's approach, Mesarovic *et al.* [19] consider an ordered field of periodically stacked pile-ups against an obstacle (i.e. interface).⁴ Each slip system carries a characteristic length, ℓ^α , interpreted as the average spacing of discrete slip planes for that slip system. These evolve with deformation, but on a timescale slower than slips. We note that these lengths are in fact associated with slip planes, rather than with slip systems, so that they need not all be independent. For example, for *fcc* crystals, at any material point, there will be only four

⁴In this case, the separate two-dimensional analysis of screw and edge components of pile-ups is justified by decoupling of screws and edge component as anti-plane and plane strain whenever such decoupling is allowed by material symmetries. In addition to isotropic elasticity, such decoupling occurs if the material symmetry group includes the mirror plane orthogonal to the dislocation line.

characteristic lengths, each covering three slip systems. The overall form has similarities with Gurtin's [2] formulation and the energy term analogous to (1.1) is a quadratic form of in-plane slip gradients for each slip system

$$\frac{1}{2} \sum_{\alpha=1}^{N_s} \sum_{\beta=1}^{N_s} \mathbf{g}^{\alpha} \cdot \mathbf{D}^{\alpha\beta} \cdot \mathbf{g}^{\beta}. \quad (3.6)$$

Rank-two constitutive tensors $\mathbf{D}^{\alpha\beta}$ have the form

$$\mathbf{D}^{\alpha\beta} = \ell^{\alpha} \ell^{\beta} \mathbf{d}^{\alpha\beta} = \ell^{\alpha} \ell^{\beta} \left[\mathbf{d}_{\perp\perp}^{\alpha\beta} \mathbf{s}^{\alpha} \mathbf{s}^{\beta} + \mathbf{d}_{\perp\circ}^{\alpha\beta} \mathbf{s}^{\alpha} \mathbf{t}^{\beta} + \mathbf{d}_{\circ\perp}^{\alpha\beta} \mathbf{t}^{\alpha} \mathbf{s}^{\beta} + \mathbf{d}_{\circ\circ}^{\alpha\beta} \mathbf{t}^{\alpha} \mathbf{t}^{\beta} \right]. \quad (3.7)$$

Clearly, $\mathbf{d}_{\perp\circ}^{\alpha\beta} = \mathbf{d}_{\circ\perp}^{\beta\alpha}$, so that

$$\mathbf{D}^{\alpha\beta} = \left[\mathbf{D}^{\beta\alpha} \right]^{\text{T}}. \quad (3.8)$$

It will be shown shortly that this symmetry is equivalent to (2.1).

The length-free components $\mathbf{d}_{XY}^{\alpha\beta}$ are proportional to elastic constants and depend on the relative orientation of the two systems (see §6a). While explicitly derived only for isotropic elasticity [19], it is clear that the general form of (3.7) will be the same for the anisotropic case,⁵ except that the components $\mathbf{d}_{XY}^{\alpha\beta}$ will depend not only on the relative orientation of the two systems, but also on their orientation with respect to the canonical crystal basis.

The physical interpretation of additional energy terms (3.6) is the *coarsening error* in interaction energy of dislocations. More precisely, it is the difference in energy computed from discrete dislocations as line defect, and the energy computed from the kinematically equivalent, smooth Nye's fields. Proper interpretation of Groma's analysis leads to the same physical interpretation of additional energy (3.1). We emphasize that the interaction energy of dislocations *represented as continuous densities* is included in the simple (size-independent) elastic-plastic continuum as the strain energy associated with incompatible elastic strains [27,28]. What remains is the energy error caused by smoothing out discrete dislocations into density fields. Moreover, this energy error is localized to the region of the size comparable to the characteristic length (i.e. they are short-range). The irreducibly non-local portion of dislocation interactions (i.e. the long-range interactions) is entirely contained within the classic size-independent elastic-plastic continuum.

4. Connection between physical and phenomenological theories

Whether one considers random or ordered dislocations arrays, with multiple lengths or a single one, it is clear that the energy expressed in terms of densities, either (3.1) or (3.6), must be regarded as the proper physical basis for the energy expressed in terms of Nye's components (1.1). If Nye's tensor \mathbf{A} allowed a unique deconstruction into densities $\{(\rho b)^I\}$ (1.2) or $\{\mathbf{g}^{\alpha}\}$ (3.4), the analysis would be simple; substitution of such linear inverses into either (3.1) or (3.6) would yield the unique values for the components of tensor \mathbf{M} in (1.1) in terms of $[K]$, or $\mathbf{D}^{\alpha\beta}$. However, in addition to physical ambiguity of pseudo-inversion of (1.2) on the basis of norm minimization, the resulting pseudo-inverse relations are nonlinear and do not yield a unique \mathbf{M} in (1.1). Therefore, it is of interest to understand in what sense (1.1) approximates the physical expressions (3.1) and (3.6), as well as if there are any special cases when the representation (1.1) is correct.

In trying to reconcile (3.6) and (1.1), it is convenient to use a somewhat different formulation of (1.1): $\mathbf{A}^{\text{T}} : \bar{\mathbf{M}} : \mathbf{A}$, where the components of $\bar{\mathbf{M}}$ are obtained by simply switching the first

⁵Any rank-2 tensor can be represented on a dual basis, say $(\mathbf{s}, \mathbf{m}, \mathbf{t})^{\alpha, \beta}$. The quadratic form (3.6) of vectors lying in slip planes α and β makes all components with dyads involving \mathbf{m}^{α} or \mathbf{m}^{β} energetically impotent, so that only components included in (3.7) remain.

two indices of \mathbf{M} . Then, upon equating (1.1) and (3.6), and substituting (3.7) into this equality, we obtain

$$\sum_{\alpha=1}^{N_S} \sum_{\beta=1}^{N_S} \mathbf{g}^\alpha \cdot \mathbf{D}^{\alpha\beta} \cdot \mathbf{g}^\beta = - \sum_{\alpha=1}^{N_S} \sum_{\beta=1}^{N_S} \mathbf{g}^\alpha \cdot [\mathbf{m}^\alpha \times (\mathbf{s}^\alpha \cdot \bar{\mathbf{M}} \cdot \mathbf{s}^\beta) \times \mathbf{m}^\beta] \cdot \mathbf{g}^\beta. \quad (4.1)$$

The equality (4.1) is valid for arbitrary combination of vectors \mathbf{g}^α , so that

$$\mathbf{D}^{\alpha\beta} = -\mathbf{m}^\alpha \times (\mathbf{s}^\alpha \cdot \bar{\mathbf{M}} \cdot \mathbf{s}^\beta) \times \mathbf{m}^\beta; \quad \alpha, \beta = 1, \dots, N_S. \quad (4.2)$$

Upon transforming the symmetry relation (2.1) into

$$\bar{M}_{ijkl} = M_{jikl} = M_{klji} = \bar{M}_{lkji},$$

it is easily shown that symmetries (3.8) and (2.1) are equivalent.

Thus, there are $N_S(N_S + 1)/2$ tensor equations (3.7), or $2N_S(N_S + 1)$ scalar conditions, which are to be satisfied by no more than 45 independent components \mathbf{M} . For *fcc* crystals with 12 slip systems, the number of scalar conditions is 312. As material symmetries impose additional restrictions on \mathbf{M} , the slip system geometry also imposes additional restrictions on $\mathbf{D}^{\alpha\beta}$. This problem is addressed in §5.

Should the multiplicity of length scales be discarded (either for physical reasons or for mathematical convenience), there would be a reduction in the number of independent material constants. From (3.5), for each pair of slip planes that share slip direction, α and α' ,

$$d_{\odot X}^{\alpha\beta} = d_{\odot X'}^{\alpha'\beta}; \quad X = \odot, \perp. \quad (4.3)$$

An analysis, analogous to the one leading to (4.2), can be applied to the other definition of the size-dependent energy (3.1), yielding

$$K^{IJ} = \xi^I \cdot (\mathbf{s}^I \cdot \bar{\mathbf{M}} \cdot \mathbf{s}^J) \cdot \xi^J = (\xi \mathbf{s})^I : \bar{\mathbf{M}} : (\mathbf{s} \xi)^J; \quad I, J = 1, \dots, N_T \quad (4.4)$$

With symmetric $[K]$ and \mathbf{M} , the maximum number of independent conditions (4.4) is $N_T(N_T + 1)/2$ (171 for *fcc*). The reduction in the number of independent scalar conditions, from (4.2) to (4.4), is accompanied by the loss of multiplicity of characteristic lengths.

At first sight, it does not appear that the phenomenological energy (1.1) can represent the physical expressions (3.1) or (3.6). Nevertheless, we proceed with the analysis, in the hope of understanding the approximation introduced by the phenomenological energy. To that end, we first expand (4.2) into scalar edge–screw interactions. Upon substituting $\mathbf{m} = \mathbf{t} \times \mathbf{s}$ in (4.2) and using $\varepsilon - \delta$ equality

$$\left. \begin{aligned} D_{\perp\perp}^{\alpha\beta} &= (\mathbf{st})^\alpha : \mathbf{M} : (\mathbf{st})^\beta = M_{jikl} s_i^\alpha t_j^\alpha t_k^\beta s_l^\beta; \\ D_{\perp\odot}^{\alpha\beta} &= -(\mathbf{ts})^\alpha : \mathbf{M} : (\mathbf{ss})^\beta = -M_{jikl} s_i^\alpha t_j^\alpha s_k^\beta s_l^\beta; \\ D_{\odot\perp}^{\alpha\beta} &= -(\mathbf{ss})^\alpha : \mathbf{M} : (\mathbf{st})^\beta = -M_{jikl} s_i^\alpha s_j^\alpha t_k^\beta s_l^\beta; \\ D_{\odot\odot}^{\alpha\beta} &= (\mathbf{ss})^\alpha : \mathbf{M} : (\mathbf{ss})^\beta = M_{jikl} s_i^\alpha s_j^\alpha s_k^\beta s_l^\beta. \end{aligned} \right\} \quad (4.5)$$

5. Additional symmetries of slip systems

To determine the number of independent parameters $d_{XY}^{\alpha\beta}$ ($X, Y = \perp, \odot$) in (3.7), and thus (with a single length scale), the number of independent conditions (4.2), (4.4)), we consider symmetries in the slip system geometry. Most material symmetry groups contain rotations and mirror reflection. The summary of the most important rules is as follows.

1. For a *family of slip systems* (i.e. the set of slip systems obtained by applying the symmetry operations on a single slip system), it is sufficient to count independent interactions of a single slip system with other slip system. All other interaction coefficients are dependent, i.e. obtainable by application of a symmetry operation.

2. Moreover, if the system β can be obtained from the system α by applying symmetry operations which are in the material symmetry group, then the interaction between α -screw and β -edge is identical to the interaction between α -edge and β -screw, i.e. $d_{\odot\perp}^{\alpha\beta} = d_{\odot\perp}^{\beta\alpha}$, so that the interaction matrices are symmetric:

$$\mathbf{D}^{\alpha\beta} = \left[\mathbf{D}^{\alpha\beta} \right]^T. \quad (5.1)$$

Consequently, only three of four components of $\mathbf{D}^{\alpha\beta}$ are independent. We emphasize that this is only true within a family of slip systems.

Let the systems (β, Y) and (β', Y') be mirror images with respect to the mirror plane m .

3. If m is orthogonal to the dislocation line (α, X) :

$$d_{\perp Y}^{\alpha\beta} = d_{\perp Y'}^{\alpha\beta'} \quad (m \perp \xi) \quad (5.2)$$

and

$$d_{\odot Y}^{\alpha\beta} = -d_{\odot Y'}^{\alpha\beta'} \quad (m \perp \xi). \quad (5.3)$$

4. If m is parallel to the dislocation line (α, X) :

$$d_{\odot Y}^{\alpha\beta} = d_{\odot Y'}^{\alpha\beta'} \quad (m \parallel \xi) \quad (5.4)$$

and

$$d_{\perp Y}^{\alpha\beta} = d_{\perp Y'}^{\alpha\beta'} \quad (m \parallel \xi \wedge m \perp \mathbf{b}). \quad (5.5)$$

Note that the last rule (5.5) requires that the mirror plane be orthogonal to the edge Burgers vector, which, in general, need not be the case.

5. Finally, if one of the screws lies in the mirror plane and the other is orthogonal to that plane, their interaction vanishes.

(a) *Fcc* slip systems

The $\{111\}/\langle\bar{1}10\rangle$ family of *fcc* slip systems is easily visualized as a regular octahedron (figure 1a) with each slip plane represented twice. To count the independent energy coefficients, we enumerate slip planes as A, B, C and D , each having three slip systems, as shown in figure 1b. We then count the independent interactions with the slip system $A1$. The relevant mirror planes are shown in figure 1c. The rule (1) reduces the number of independent interaction coefficients to 36. This number is further reduced by application of the mirror rules (5.3)–(5.5) to 13, listed in table 1. There are only two independent interactions between the screws, four independent screw–edge interactions (including the interactions within the same slip plane), and seven independent edge–edge interactions. The last number is the largest, because there are no mirror planes orthogonal to the edge dislocation lines, so that (5.2) is not applicable.

(b) *Bcc* slip systems

The $\{110\}/\langle\bar{1}11\rangle$ family of slip systems consists of six slip planes, each hosting two slip directions. Screw dislocations lie in the mirror planes, so that (5.4) applies. Rules (1) and (2) apply, so we consider only interactions of one slip system.

The four possible screws give three independent screw–screw interactions: self + pair of mirrored screws +1. There are 12 edges, giving seven independent screw–edge interactions: five mirrored pairs + within the same plane +1. Edge–edge interactions are not subjected to any symmetry reductions, so that their number is 12. The total number of independent interactions, for the $\{110\}/\langle\bar{1}11\rangle$ family alone, is 22.

The $\{211\}/\langle\bar{1}11\rangle$ family of slip systems consists of 12 slip planes, each hosting one slip direction. The same symmetry (5.4) applies, so that the total number of independent interactions within this slip system family is also 22.

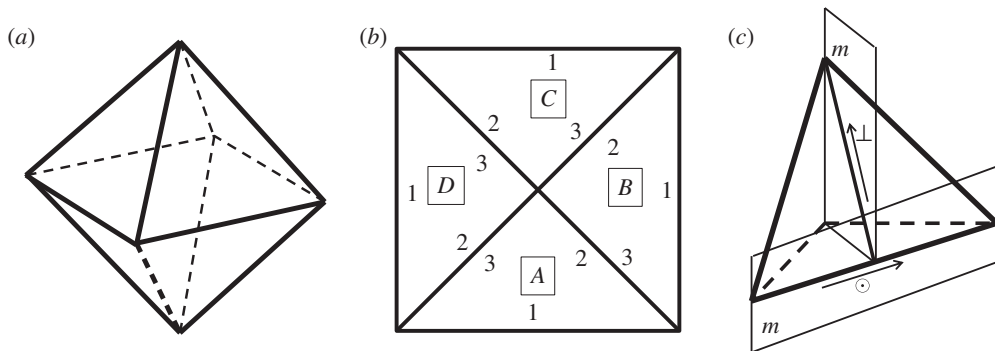


Figure 1. (a) Geometry of fcc slip planes: four slip planes form a half of the regular octahedron. Edges are slip directions. (b) Top view of the octahedron with enumeration of slip systems. (c) One slip plane with directions of screw and edge dislocations and relevant mirror planes (m), corresponding to the rules (5.3)–(5.5) in the text.

Table 1. Independent energy coefficients for the $\{111\}/\langle\bar{1}10\rangle$ family of slip systems in an fcc crystal. The slip system ordering (A1–D3) is shown in figure 1b. The numbers reflect the arbitrary order in which the interactions have been considered, except 0 which signifies vanishing interaction.

	A1	A2	A3	B1	B2	B3	C1	C2	C3	D1	D2	D3	total
$\odot\odot$	1	2	2	0	2	2	1	2	2	0	2	2	2
$\odot\perp$	3	4	4	5	6	6	3	4	4	5	6	6	4
$\perp\perp$	7	8	8	9	10	11	12	13	13	9	11	10	7

If both families are active, the number of interactions is much larger, but owing to the condition (5.4), smaller than the nominal number. With four screws and 24 edges, the nominal number is $N_T(N_T + 1)/2 = 406$.

6. Computation of the size-dependent energy by coarsening the discrete dislocation energies

In previous sections, we attempted to deduce the number of independent constants required to compute dislocation interactions, solely on the basis of crystal and slip symmetries. The purpose of this analysis is to determine whether a global representation of size-dependent energy (1.1) in terms of Nye's field represents the physical theories. Based on such discussion, the answer to the above question is negative. In general, the global representation (1.1) is not equivalent to the physical models (3.1) and (3.6), *not even if all the characteristic lengths of various slip systems are equal*.

Thus far, we have not addressed the question of how may the constitutive tensors, \mathbf{M} (1.1) and $\mathbf{D}^{\alpha\beta}$ (3.6), or the constitutive matrix $[K]$ (3.1), be computed. To compute the size-dependent energy from dislocation mechanics, some form of spatial coarsening method is required. In other words, any local representation of size-dependent energy, such as (3.1) or (3.6), is necessarily a local approximation to the exact (within the discrete dislocation mechanics) non-local form. The approximation method is likely to include additional symmetries, so that the question of equivalence between the phenomenological (1.1) and physical (3.1, 3.6) expressions of size-dependent energy must be reconsidered.

To that end, we first write a more explicit mathematical description of the physical interpretation of the size-dependent energy as the coarsening error in dislocation interaction energies. Consider a continuum (coarse) description of dislocations. Dislocations of type α are

characterized by continuum field ρ^α , its Burgers vector $b^\alpha \mathbf{s}^\alpha$, and its line direction ξ^α . The interaction energy of the two types of dislocations can be represented as

$$E_{\text{coarse}}^{\alpha\beta} = \frac{1}{2} \int_V dV^\alpha \int_V dV^\beta \frac{(\rho b)^\alpha (\rho b)^\beta}{R} (\mathbf{s}^\alpha \xi^\alpha) : \mathbf{L} : (\xi^\beta \mathbf{s}^\beta), \quad (6.1)$$

where $dV^\alpha = dx_1^\alpha dx_2^\alpha dx_3^\alpha$, $R = |\mathbf{R}|$, $\mathbf{R} = \mathbf{x}^\beta - \mathbf{x}^\alpha$, whereas the rank-four two-point tensor field \mathbf{L} is a function of the direction $\mathbf{r} = \mathbf{R}/R$: $\mathbf{L}(\mathbf{r})$. Such expression has been derived for isotropic elasticity [27,29]. Owing to the complexity of anisotropic interactions, an explicit expression (6.1) for the anisotropic case has not been formulated. In §6*b*, we show that such expression can, in principle, be derived. In §6*c*, we provide some details for the case of cubic symmetries.

Consider now the discrete description of dislocations, $\hat{\rho}^\alpha$, characterized formally as a set of three-dimensional Dirac delta functions⁶. The expression for interaction energy is analogous to (6.1)

$$E_{\text{discrete}}^{\alpha\beta} = \frac{1}{2} \int_V dV^\alpha \int_{dV^\beta} \frac{(\hat{\rho} b)^\alpha (\hat{\rho} b)^\beta}{R} (\mathbf{s}^\alpha \xi^\alpha) : \mathbf{L} : (\xi^\beta \mathbf{s}^\beta). \quad (6.2)$$

Because the energy (6.1) is already included in the standard size-independent continuum (as the strain energy corresponding to incompatible elastic strains), the size-dependent energy, given by either (1.1), or (3.1), or (3.6), represents the difference between the ‘exact’ (discrete) energy (6.2) and the coarse energy (6.1)

$$E_{\text{discrete}}^{\alpha\beta} - E_{\text{coarse}}^{\alpha\beta} = \frac{1}{2} \int_V dV^\alpha \int_V dV^\beta \frac{(\hat{\rho} - \rho)^\alpha b^\alpha (\hat{\rho} - \rho)^\beta b^\beta}{R} (\mathbf{s}^\alpha \xi^\alpha) : \mathbf{L} : (\xi^\beta \mathbf{s}^\beta) \quad (6.3)$$

The key mathematical difference between (6.3) and (6.1)–(6.2) is that while the kernels in (6.1)–(6.2) are essentially non-local (long-range interactions), the kernel in (6.3) is localized (short-range) to the small values of R . Both physical theories discussed here [18,19] rely on that fact, albeit for different assumed arrangement of dislocations. The kernels are given explicitly and graphically in reference [19] for isotropic elasticity, single slip system and stacked pile-ups configuration⁷. While the kernels for anisotropic case and interaction between different types of dislocations have not been derived explicitly, powerful intuitive arguments indicate that the localization property holds⁸. Thus, each slip system is characterized with the characteristic length ℓ^α , such that for $R > \ell^\alpha$ the kernel in (6.3) vanishes, i.e. the interaction energies between remote dislocations are insensitive to the representation of dislocations (discrete or smeared).

Consider a RVE with volume V_{RVE} . When interpreted in view of (6.3), the representation (3.1) embodies the claim that

$$\frac{E_{\text{discrete}}^{\alpha\beta} - E_{\text{coarse}}^{\alpha\beta}}{V_{\text{RVE}}} = \frac{1}{2} (\rho b)^\alpha K^{\alpha\beta} (\rho b)^\beta. \quad (6.4)$$

⁶Alternatively, one may consider a set of sharp peaks with a certain width, which in the limit of zero width approach Dirac delta functions.

⁷For illustration of essentially non-local kernels of (6.1) and (6.2) in isotropic elasticity, see Baskaran *et al.* [30].

⁸Consider a discrete dislocation and its equivalent smeared distribution, both in an infinite elastic solid. In both cases, the interaction energies with another defect are essentially non-local, i.e. without a cut-off distance. The statement that the difference between the two cases is localized amounts to the statement that for a defect sufficiently removed from the dislocation core, the exact representation of dislocation does not affect the interaction energy.

In view of the localization property in (6.3), let the RVE be the sphere with radius $\sqrt{\ell^\alpha \ell^\beta}$. If the discrete distribution is a uniform distribution of Dirac delta functions, it seems reasonable to assume the proportionality

$$\begin{aligned} K^{\alpha\beta} &\sim \int_{V_{\text{RVE}}} dV^\alpha \int_{V_{\text{RVE}}} dV^\beta \frac{1}{R} (\mathbf{s}^\alpha \boldsymbol{\xi}^\alpha) : \mathbf{L} : (\boldsymbol{\xi}^\beta \mathbf{s}^\beta) \\ &= (\mathbf{s}^\alpha \boldsymbol{\xi}^\alpha) : \left[\int_{V_{\text{RVE}}} dV^\alpha \int_{V_{\text{RVE}}} dV^\beta \frac{1}{R} \mathbf{L} \right] : (\boldsymbol{\xi}^\beta \mathbf{s}^\beta). \end{aligned} \quad (6.5)$$

The tensor field \mathbf{L} is independent of the choice of slip systems (dislocation types) α and β , but the double integral depends on the characteristic lengths. In analogy to (4.4), we can write

$$K^{\alpha\beta} = (\mathbf{s}^\alpha \boldsymbol{\xi}^\alpha) : \bar{\mathbf{M}}^{\alpha\beta} : (\boldsymbol{\xi}^\beta \mathbf{s}^\beta); \quad \bar{\mathbf{M}}^{\alpha\beta} \sim \frac{1}{2} \int_{V_{\text{RVE}}} dV^\alpha \int_{V_{\text{RVE}}} dV^\beta \frac{1}{R} \mathbf{L}(\mathbf{r}). \quad (6.6)$$

For the spherical RVE, the integrals over distance and direction separate. Let S_0 be the surface of the unit sphere. Then

$$\bar{\mathbf{M}}^{\alpha\beta} \sim \ell^\alpha \ell^\beta \int_{S_0} d\mathbf{S} \mathbf{L}(\mathbf{r}). \quad (6.7)$$

It is clear that the tensor $\bar{\mathbf{M}}$, as defined in (4.4), cannot exist in the general case. However, if the characteristic lengths are assumed equal, $\ell^\alpha = \ell$ for all α , the expression

$$\bar{\mathbf{M}} \sim \ell^2 \int_{S_0} d\mathbf{S} \mathbf{L}(\mathbf{r}), \quad (6.8)$$

provides a recipe for computing $\bar{\mathbf{M}}$ (or \mathbf{M}). Although conceptually simple and easily implemented for isotropic elasticity, the computations are significantly more complicated in the anisotropic case.

We first consider the case of elastic isotropy. Then, we return to the general anisotropic case in §6b, where we discuss the properties of the tensor $\bar{\mathbf{M}}$ obtained by the averaging procedure described in this section and leading to (6.8).

(a) Elastically isotropic crystal

To analyse the isotropic case, we substitute the isotropic tensor \mathbf{M} (2.4) into (4.5)

$$\left. \begin{aligned} D_{\perp\perp}^{\alpha\beta} &= M_2(\mathbf{s}^\alpha \cdot \mathbf{t}^\beta)(\mathbf{t}^\alpha \cdot \mathbf{s}^\beta) + M_3(\mathbf{s}^\alpha \cdot \mathbf{s}^\beta)(\mathbf{t}^\alpha \cdot \mathbf{t}^\beta); \\ D_{\perp\circ}^{\alpha\beta} &= -(M_2 + M_3)(\mathbf{s}^\alpha \cdot \mathbf{s}^\beta)(\mathbf{t}^\alpha \cdot \mathbf{s}^\beta); \\ D_{\circ\perp}^{\alpha\beta} &= -(M_2 + M_3)(\mathbf{s}^\alpha \cdot \mathbf{s}^\beta)(\mathbf{s}^\alpha \cdot \mathbf{t}^\beta) \\ D_{\circ\circ}^{\alpha\beta} &= M_1 + (M_2 + M_3)(\mathbf{s}^\alpha \cdot \mathbf{s}^\beta)^2. \end{aligned} \right\} \quad (6.9)$$

and

In the isotropic case, the tensor \mathbf{L} is computed as [27]

$$L_{ijkl} \sim 2\mu(2\delta_{ik}\delta_{jl} - \delta_{ij}\delta_{kl}) - \bar{E}(\delta_{ik}\delta_{jl} - \delta_{il}\delta_{jk}) - \epsilon_{mij} r_m r_n \epsilon_{nkl}, \quad (6.10)$$

where μ is the shear modulus, \bar{E} is the plane strain modulus, $\bar{E} = 2\mu/(1 - \nu)$, with ν being the Poisson ratio.

Mesarovic *et al.* [19] derived the size-dependent energy for dislocations belonging to the same slip system

$$\frac{1}{2} \mathbf{g}^\alpha \cdot \mathbf{D}^{\alpha\alpha} \cdot \mathbf{g}^\alpha, \quad (6.11)$$

with

$$D_{\perp\perp}^{\alpha\alpha} = \ell^\alpha \ell^\alpha \frac{\bar{E}}{12}, \quad D_{\circ\circ}^{\alpha\alpha} = \ell^\alpha \ell^\alpha \frac{\mu}{12}, \quad D_{\circ\perp}^{\alpha\alpha} = D_{\perp\circ}^{\alpha\alpha} = 0. \quad (6.12)$$

Then, using proportionality (6.7), and noting that upon integration the last term in (6.10) vanishes, we obtain⁹

$$\left. \begin{aligned} D_{\perp\perp}^{\alpha\beta} &= \ell^\alpha \ell^\beta \frac{\bar{E}}{12} (\mathbf{s}^\alpha \cdot \mathbf{s}^\beta) (\mathbf{t}^\alpha \cdot \mathbf{t}^\beta) + \ell^\alpha \ell^\beta \frac{2\mu - \bar{E}}{12} (\mathbf{s}^\beta \cdot \mathbf{t}^\alpha) (\mathbf{s}^\alpha \cdot \mathbf{t}^\beta); \\ D_{\perp\circ}^{\alpha\beta} &= -\ell^\alpha \ell^\beta \frac{2\mu}{12} (\mathbf{s}^\alpha \cdot \mathbf{s}^\beta) (\mathbf{t}^\alpha \cdot \mathbf{s}^\beta); \\ D_{\circ\perp}^{\alpha\beta} &= -\ell^\alpha \ell^\beta \frac{2\mu}{12} (\mathbf{s}^\alpha \cdot \mathbf{s}^\beta) (\mathbf{s}^\alpha \cdot \mathbf{t}^\beta) \\ \text{and} \quad D_{\circ\circ}^{\alpha\beta} &= \ell^\alpha \ell^\beta \frac{2\mu}{12} \left[(\mathbf{s}^\alpha \cdot \mathbf{s}^\beta)^2 - \frac{1}{2} \right]. \end{aligned} \right\} \quad (6.13)$$

Comparison between (6.9) and (6.13) gives a triplet of coefficients for each pair of slip systems

$$M_1^{\alpha\beta} = \ell^\alpha \ell^\beta \frac{\mu}{12}; \quad M_2^{\alpha\beta} = \ell^\alpha \ell^\beta \frac{2\mu - \bar{E}}{12}; \quad M_3^{\alpha\beta} = \ell^\alpha \ell^\beta \frac{\bar{E}}{12}. \quad (6.14)$$

Clearly, these do not form a unique tensor \mathbf{M} (2.4) in the general case. However, if the characteristic lengths are identical, we obtain

$$M_1 = \frac{\ell^2}{12} \mu; \quad M_2 = \frac{\ell^2}{12} (2\mu - \bar{E}); \quad M_3 = \frac{\ell^2}{12} \bar{E}. \quad (6.15)$$

Moreover, only two of three coefficients in (2.4) are independent

$$M_2 = 2M_1 - M_3 \quad (6.16)$$

and

$$M_{ijkl} = \frac{\mu \ell^2}{12} (\delta_{ij} \delta_{kl} + 2\delta_{jk} \delta_{li}) + \frac{\bar{E} \ell^2}{12} (\delta_{jl} \delta_{ik} - \delta_{jk} \delta_{li}). \quad (6.17)$$

In summary, for the case of elastic isotropy and a single characteristic length, the phenomenological energy representation (1.1) corresponds to the physical representation (3.6).

It is instructive to contrast the reduction in the number of independent constants from 3 to 2 for tensors \mathbf{M} and \mathbf{C} . The elasticity tensor \mathbf{C} has only two independent constants because it possesses the minor symmetry: $C_{IJKL} = C_{JKLI} = C_{ILJK}$. With reference to (2.3), this implies $C_2 \equiv C_3$. However, the tensor \mathbf{M} (6.17) does not possess the minor symmetry. The reduction in the number of independent coefficients (6.16) follows from dimensional analysis and its dependence on \mathbf{C} .

(b) Anisotropic crystal

Consider two dislocation segments, α and β , with Burgers vectors $b^\alpha \mathbf{s}^\alpha$ and $b^\beta \mathbf{s}^\beta$. Let infinitesimal segments vectors $d\mathbf{x}^\alpha \boldsymbol{\xi}^\alpha$ and $d\mathbf{x}^\beta \boldsymbol{\xi}^\beta$ be located at \mathbf{x}^α and \mathbf{x}^β (figure 2). Define

$$\mathbf{R} = \mathbf{x}^\beta - \mathbf{x}^\alpha; \quad R = |\mathbf{R}|; \quad \mathbf{r} = \frac{\mathbf{R}}{R}. \quad (6.18)$$

In the plane orthogonal to the unit vector \mathbf{r} , choose an arbitrary direction and define the unit vector $\mathbf{n}(\phi)$, where ϕ is measured from the chosen direction.

⁹The coefficients in (6.13) have been derived in reference [19], but for a different convention, and with an error in the edge-edge interactions. Here, we correct the error and give results for the convention used in this paper: $\boldsymbol{\xi}_\circ^\alpha = \mathbf{s}^\alpha$, $\boldsymbol{\xi}_\perp^\alpha = -\mathbf{t}^\alpha$.

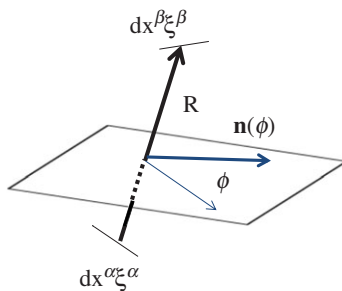


Figure 2. Geometry for interaction of two infinitesimal dislocation segments located at \mathbf{x}^α and \mathbf{x}^β . (Online version in colour.)

From the major symmetry and positive definiteness of the elasticity tensor \mathbf{C} , it follows that the rank-two tensor

$$\mathcal{M} = \mathbf{n} \cdot \mathbf{C} \cdot \mathbf{n}, \quad (6.19)$$

is symmetric and positive definite. Next, define the rank-four tensor

$$\mathcal{L} = \mathbf{n} \times [(\mathbf{C} \cdot \mathbf{n}) \cdot \mathcal{M}^{-1} \cdot (\mathbf{n} \cdot \mathbf{C}) - \mathbf{C}] \times \mathbf{n}. \quad (6.20)$$

The elementary interaction between two infinitesimal segments can be written as [31,32]

$$\frac{1}{8\pi^2} \frac{b^\alpha dx^\alpha b^\beta dx^\beta}{R} (\mathbf{s}^\alpha \xi^\alpha) : \left[\int_0^{2\pi} \mathcal{L} d\varphi \right] : (\xi^\beta \mathbf{s}^\beta). \quad (6.21)$$

The integration domain in (6.21) is the unit circle in the plane shown in figure 2, which we denote c_0 . Then, following (6.5) to (6.8), we write

$$\mathbf{L}(\mathbf{C}, \mathbf{r}) \sim \int_{c_0} \mathcal{L}(\mathbf{C}, \mathbf{r}, \mathbf{n}) d\varphi; \quad \bar{\mathbf{M}}(\mathbf{C}) \sim \ell^2 \int_{S_0} dS \int_{c_0} d\varphi \mathcal{L}(\mathbf{C}, \mathbf{r}, \mathbf{n}). \quad (6.22)$$

The second equation corresponds to the case where all characteristic lengths are identical. Integral over the unit circle c_0 is the integral over all directions \mathbf{n} in the plane shown in figure 2, whereas in the outer integral over the unit sphere S_0 is the integral over all spatial directions \mathbf{r} .

From (6.19) and (6.20), the tensor \mathcal{L} is a homogeneous function of order 1 of the tensor \mathbf{C} :

$$\mathcal{L}(\lambda \mathbf{C}, \mathbf{r}, \mathbf{n}) = \lambda \mathcal{L}(\mathbf{C}, \mathbf{r}, \mathbf{n}). \quad (6.23)$$

The integration over directions \mathbf{r} and \mathbf{n} in (6.22) does not affect the homogeneity, so that the tensor $\bar{\mathbf{M}}$ is also a homogeneous function of order 1 of \mathbf{C} :

$$\bar{\mathbf{M}}(\lambda \mathbf{C}) = \lambda \bar{\mathbf{M}}(\mathbf{C}). \quad (6.24)$$

Let the symmetry operation \mathbf{Q} be in the material symmetry group, so that the components of \mathbf{C} are invariant under this symmetry operation

$$\langle \mathbf{Q} \rangle^4 * \mathbf{C} = \mathbf{C}. \quad (6.25)$$

Then, with $\lambda = 1$ in (6.24)

$$\bar{\mathbf{M}}(\langle \mathbf{Q} \rangle^4 * \mathbf{C}) = \bar{\mathbf{M}}(\mathbf{C}). \quad (6.26)$$

Thus, $\bar{\mathbf{M}}$ is invariant under all transformations that leave \mathbf{C} invariant. In appendix A, we show that the tensor $\bar{\mathbf{M}}$ transforms in a manner that satisfies the principle of material frame indifference (2.2) for rank-four tensors, i.e.

$$\bar{\mathbf{M}}(\langle \mathbf{Q} \rangle^4 * \mathbf{C}) = \langle \mathbf{Q} \rangle^4 * \bar{\mathbf{M}}(\mathbf{C}). \quad (6.27)$$

Therefore, if all the characteristic lengths are equal, the tensor $\bar{\mathbf{M}}$ (6.8) is uniquely defined, so that in this case, the phenomenological expression (1.1) is justified.

Moreover, we expect the tensor $\bar{\mathbf{M}}$ to have the same number of independent constants as \mathbf{C} , for the same reason as in the isotropic case, cf. discussion after (6.17). However, we were unable to prove that the relationship which reduces the number of independent constants, such as (6.16) for isotropic case, is linear in the general case. The difficulty lies in the fact that order 1 homogeneity (6.23)–(6.24) between a tensor and its tensor function does not imply linear relationship between the components of the two tensors.

As an aside, we prove in appendix B that the tensor $\bar{\mathbf{M}}$ satisfies the index *reversal* symmetry

$$\bar{M}_{ijkl} = \bar{M}_{lkji}, \quad (6.28)$$

for any symmetry group. While isotropic and cubic symmetry groups (S2) include this symmetry, other symmetry groups do not¹⁰. Assuming that the major symmetry is given, the reversal symmetry follows from the minor symmetry, but the converse is not true.

If the characteristic lengths are not equal, we rewrite (6.7) as

$$\bar{\mathbf{M}}^{\alpha\beta}(\mathbf{C}) \sim \ell^\alpha \ell^\beta \bar{\mathbf{m}}(\mathbf{C}); \quad \bar{\mathbf{m}}(\mathbf{C}) = \int_{S_0} dS \int_{c_0} dc \mathcal{L}(\mathbf{C}, \mathbf{r}, \mathbf{n}). \quad (6.29)$$

Now, the tensor $\bar{\mathbf{m}}$ inherits all the symmetries (and the number of independent constants) from the elasticity tensor \mathbf{C} , but there is no unique tensor $\bar{\mathbf{M}}$ (nor \mathbf{M}). Thus, the phenomenological expression (1.1) as quadratic form of Nye's densities cannot be physically justified in this case.

(c) Cubic crystals

In the case of cubic crystal, three independent elastic constants are required (2.5). Assume that the interactions within one slip system are known

$$D_{\perp\perp}^{\alpha\alpha} = \ell^\alpha \ell^\alpha d_{\perp\perp}, \quad D_{\odot\odot}^{\alpha\alpha} = \ell^\alpha \ell^\alpha d_{\odot\odot}, \quad D_{\odot\perp}^{\alpha\alpha} = D_{\perp\odot}^{\alpha\alpha} = \ell^\alpha \ell^\alpha d_{\perp\odot}. \quad (6.30)$$

The three coefficients: $d_{\perp\perp}$, $d_{\odot\odot}$ and $d_{\perp\odot}$, and the proportionality (6.7), are sufficient to compute all interaction matrices $\mathbf{D}^{\alpha\beta}$, provided that all characteristic lengths are known. Moreover, if all characteristic lengths are identical, the global representation in terms of Nye's fields (1.1) applies. The computation of (6.29) is the most involved step. The details of such computations for isotropic case are given in references [19,30]. In summary, this amounts to computing both energy of discrete dislocation assembly and its continuous representation, then approximating the thus obtained non-local difference by a local expression. Assuming that such result is available, it remains to perform integration (6.22). From (2.5) and (6.19)

$$\mathcal{M} = C_0 \sum_{\alpha=1}^3 n_\alpha^2 \mathbf{e}_\alpha \mathbf{e}_\alpha + (C_1 + C_2) \mathbf{nn} + C_2 \mathbf{p}_j \mathbf{p}_j \quad (6.31)$$

The simplest method to compute the inverse appears to be the application of the Cayley–Hamilton theorem

$$\mathcal{M}^{-1} = \frac{1}{\det \mathcal{M}} (\mathcal{M}^2 - I\mathcal{M} + III\mathbf{I}); \quad I = \text{tr} \mathcal{M}; II = \frac{1}{2} (I^2 - \text{tr} \mathcal{M}^2). \quad (6.32)$$

The determinant is computed as

$$\begin{aligned} \det \mathcal{M} = & C_2^2 (C_0 + C_1 + 2C_2) + C_2 C_0 (C_0 + 2C_1 + 2C_2) (n_1^2 n_2^2 + n_2^2 n_3^2 + n_3^2 n_1^2) \\ & + C_0^2 (C_0 + 3C_1 + 3C_2) n_1^2 n_2^2 n_3^2, \end{aligned} \quad (6.33)$$

¹⁰The reversal $jk \rightarrow kj$ is in fact invariance to the rotation by $\pi/2$ (or identity if $j = k$), which is included in the cubic and isotropic groups, but not in all the symmetry groups.

where the components of \mathbf{n} are in the canonical crystal system: $\mathbf{n} = n_i \mathbf{e}_i$. The integral

$$\int_0^{2\pi} [\mathbf{n} \times [(\mathbf{C} \cdot \mathbf{n}) \cdot \mathcal{M}^{-1} \cdot (\mathbf{n} \cdot \mathbf{C}) - \mathbf{C}] \times \mathbf{n}] d\phi, \quad (6.34)$$

can now be computed by means of (6.32)–(6.33) and with \mathbf{C} given by (2.5). To that end, the vector \mathbf{n} can be described in the local coordinate system

$$\left. \begin{aligned} \mathbf{p}_3 = \mathbf{r}; \quad \mathbf{n} = \cos \phi \mathbf{p}_1 + \sin \phi \mathbf{p}_2 \\ n_i = \cos \phi p_{1i} + \sin \phi p_{2i}; \quad p_{ji} = \mathbf{p}_j \cdot \mathbf{e}_i; \quad \mathbf{p}_j = p_{ji} \mathbf{e}_i. \end{aligned} \right\} \quad (6.35)$$

7. Summary and discussion—the relevance of multiple length scales

In this paper, we have addressed two questions relevant for development of size-dependent plasticity theory:

1. Can the phenomenological expression for size-dependent energy $1/2 \mathbf{A} : \mathbf{M} : \mathbf{A}$ represent the physical expressions (i.e. derived from dislocation mechanics): $1/2 \{\rho b\}^T [K] \{\rho b\}$, or equivalently, $\frac{1}{2} \sum_{\alpha} \sum_{\beta} \mathbf{g}^{\alpha} \cdot \mathbf{D}^{\alpha\beta} \cdot \mathbf{g}^{\beta}$, and under which conditions?
2. How can physical or phenomenological expressions for size-dependent energy be computed from dislocation mechanics?

The answer to the first question, based solely on the analysis of material and slip symmetries, is that the equivalence between the phenomenological and physical expressions is not possible, even if the multiplicity of characteristic lengths is sacrificed. The physical expressions require much larger number of independent constants than the number allowed to the phenomenological expression by the material symmetries.

The coarsening method developed in §6 is based on the physical interpretation of the size-dependent energy as the coarsening error in dislocation interaction energy (or, equivalently, the strain energy associated with incompatible elastic strains). It amounts to a local approximation of a non-local (but localized to a small domain) expression and includes the following assumptions:

- (A) The coarsening error in interaction between two sets of dislocations is proportional to the total energy.
- (B) The spatial averaging over the spherical RVE whose size is the geometric mean of characteristic lengths associated with the two slip systems.

Such coarsening procedure introduces additional symmetries. Nevertheless, the answer to the first question is still negative for the general case. However, if all characteristic lengths are equal, the equivalence between phenomenological and physical expressions is possible. Moreover, the number of independent coefficients in the phenomenological expression is lower than the one predicted by material symmetries.

Given the mathematical convenience of the phenomenological expression, the question of error incurred by assuming that all slip systems have the same characteristic length, deserves some consideration. In Mesarovic *et al.* [19], the physical interpretation of the characteristic length of a slip system is the average spacing between the stacked pile-ups of dislocations. Each characteristic length evolves with plastic deformation, as illustrated in figure 3*a*. In early stages of deformation of a well-annealed crystal, the characteristic length is determined by the average spacing between the Frank–Read sources. With continuing deformation, dislocation multiplication by the double cross-slip mechanism introduces a new—typically much smaller—spacing, so that the spacing distribution between stacked pile-ups is bi-modal in the intermediate stages of deformation. In the later stages, the characteristic double cross-slip distance dominates. If the second slip system is activated at later stages of deformation, the two characteristic lengths will be very different, as shown in figure 3*b*.

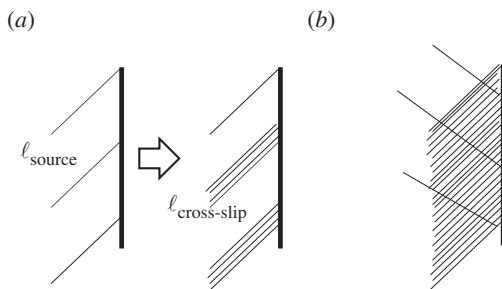


Figure 3. Pile-ups at a crystal boundary. (a) Evolution of the characteristic length for single slip. (b) Activation of the second slip systems at a later stage of deformation leads to a large difference in characteristic lengths associated with the two systems.

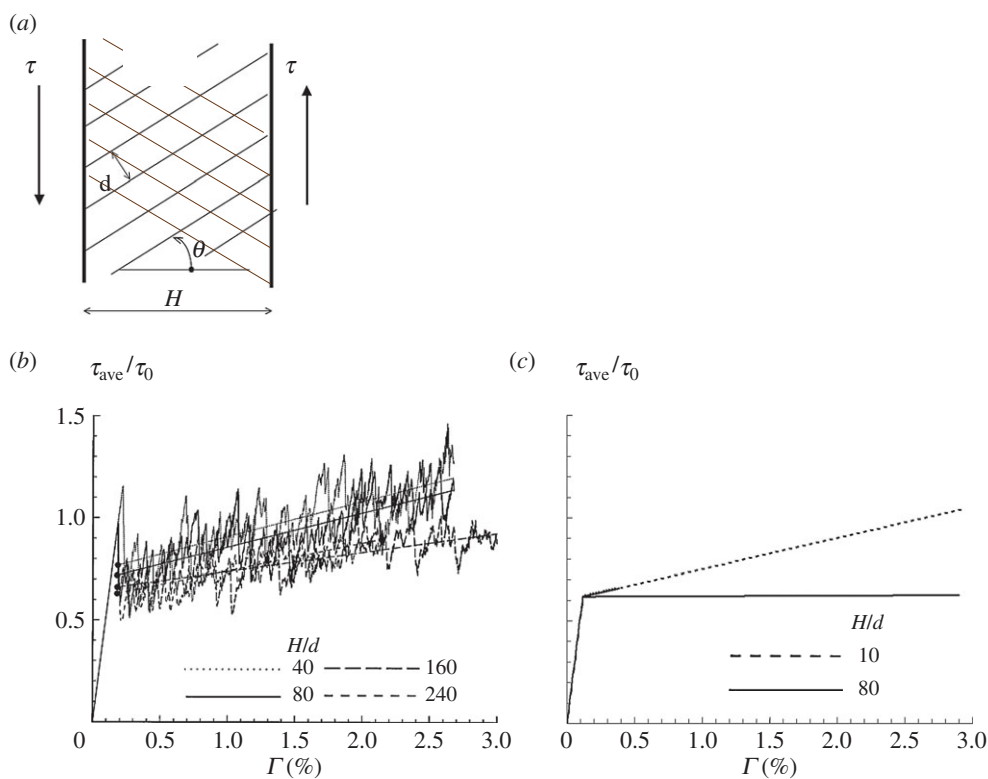


Figure 4. (a) Configuration of the thin film with symmetric double slip. Stress–strain graphs for various characteristic lengths: (b) Discrete dislocation dynamics [33]; (c) continuum theory [34].

In small volumes where interfaces dominate, the dissipative dislocation–interface reactions (penetration, dissociation, relaxation) are critical for determining the macroscopic behaviour of materials. Computation of energy is the essential first step in determining the dissipation mechanism at the boundary. Calculations using both, discrete dislocation dynamics [33] and the continuum model [34], indicate that the length scale (i.e. the spacing between slip planes) is relevant. This is illustrated in figure 4, for the simple configuration of thin film with symmetric double slip. The characteristic length has little or no effect on the initial yield, but its effect on hardening is significant.

In summary, while the assumption of equal characteristic lengths, combined with the coarsening method proposed in §6, allows for the energy representation as the quadratic form of Nye's tensor, such representation should be used with caution, as it erases potentially important effects of dissimilar characteristic length in different slip systems.

Data accessibility. All data are included in the manuscript.

Author contributions. J.P.J. contributed proofs in the appendices and contributed to the symmetry analysis in §6*b,c*. S.F. contributed to the formulation of the problem (§3), material symmetry analysis (§2) and crystal symmetry analysis (§5). S.Dj.M. contributed to the formulation of the problem (§3), formulated the connection between the physical and phenomenological theories (§4), performed the crystal symmetry analysis (§5), formulated the coarsening method (§6) and drafted the manuscript.

Funding statement. The work of S.Dj.M. was supported in parts by: visiting professorship at Centre des Matériaux, Mines ParisTech, France; US scholar grant by Fulbright Foundation; and, the professional leave programme at Washington State University.

Conflict of interests. We have no competing interests.

Appendix A. Material frame indifference of $\bar{\mathbf{M}}$

Consider an orthogonal transformation \mathbf{Q} as a transformation of the coordinate system. The vector \mathbf{n} (figure 2) is a material vector. Thus, any transformation of the coordinate system must be accompanied by transformation of \mathbf{n}

$$\mathbf{n}' = \langle \mathbf{Q} \rangle * \mathbf{n} \quad (\text{A } 1)$$

We aim to prove that

$$\mathcal{L}(\langle \mathbf{Q} \rangle^4 * \mathbf{C}, \langle \mathbf{Q} \rangle * \mathbf{n}) = \langle \mathbf{Q} \rangle^4 * \mathcal{L}(\mathbf{C}, \mathbf{n}), \quad (\text{A } 2)$$

where

$$\mathcal{L} = \mathbf{n} \times (\mathcal{P} - \mathbf{C}) \times \mathbf{n}; \quad \mathcal{P} = (\mathbf{C} \cdot \mathbf{n}) \cdot \mathcal{M}^{-1} \cdot (\mathbf{n} \cdot \mathbf{C}); \quad \mathcal{M} = \mathbf{n} \cdot \mathbf{C} \cdot \mathbf{n}. \quad (\text{A } 3)$$

The components of the tensor \mathcal{M} transform as

$$\mathcal{M}'_{jk} = n'_i C'_{ijkl} n'_l = Q_{ix} n_x Q_{ip} Q_{jq} Q_{kr} Q_{ls} C_{pqrs} Q_{ly} n_y. \quad (\text{A } 4)$$

For orthogonal transformations, $Q_{ix} Q_{ip} = \delta_{xp}$, so that

$$\mathcal{M}'_{jk} = Q_{jq} Q_{kr} \delta_{px} n_x C_{pqrs} \delta_{sy} n_y = Q_{jq} Q_{kr} \mathcal{M}_{qr}. \quad (\text{A } 5)$$

The inverse of a tensor transforms in the same way as the original tensor, so that

$$(\mathcal{M}^{-1})'_{jk} = Q_{jq} Q_{kr} (\mathcal{M}^{-1})_{qr}. \quad (\text{A } 6)$$

Next, it is easily shown, using the orthogonality of the transformation as in (A 4)–(A 5), that

$$\mathcal{P}'_{ijkl} = Q_{ip} Q_{jq} Q_{kr} Q_{ls} \mathcal{P}_{pqrs}. \quad (\text{A } 7)$$

Then, we express the transformation of \mathcal{L}

$$\mathcal{L}'_{xjky} = \epsilon_{xmi} n'_m (\mathcal{P} - \mathbf{C})'_{ijkl} n'_l \epsilon_{ytl} = \underbrace{\epsilon_{xmi} Q_{mz} n_z Q_{ip} Q_{jq} Q_{kr} Q_{ls}}_{xp} (\mathcal{P} - \mathbf{C})_{pqrs} Q_{tw} n_w \epsilon_{ytl}. \quad (\text{A } 8)$$

Consider the expression denoted xp and multiply it by $\delta_{x\beta} = Q_{x\alpha} Q_{\beta\alpha}$:

$$\delta_{x\beta} \epsilon_{xmi} Q_{mz} Q_{ip} n_z = \epsilon_{xmi} Q_{mz} Q_{ip} Q_{x\alpha} Q_{\beta\alpha} n_z = (\det \mathbf{Q}) \epsilon_{zpa} Q_{\beta\alpha} n_z. \quad (\text{A } 9)$$

It follows that

$$\epsilon_{xmi} Q_{mz} Q_{ip} n_z = (\det \mathbf{Q}) \epsilon_{zpa} Q_{x\alpha} n_z. \quad (\text{A } 10)$$

Applying the similar transformation to the terms at the tail end of (A 8), we obtain

$$\epsilon_{ylt} Q_{ls} Q_{tw} n_w = (\det \mathbf{Q}) \epsilon_{swc} Q_{yc} n_w. \quad (\text{A } 11)$$

Upon substitution into (A 8)

$$\mathcal{L}'_{xjky} = (\det \mathbf{Q})^2 Q_{xa} Q_{jq} Q_{kr} Q_{yc} \epsilon_{azp} n_z (\mathbf{P} - \mathbf{C})_{pqrs} n_w \epsilon_{swc}. \quad (\text{A } 12)$$

Upon noting that $\det \mathbf{Q} = \pm 1$ for proper / improper orthogonal transformation (rotation / inversion), we obtain

$$\mathcal{L}'_{xjky} = Q_{xa} Q_{jq} Q_{kr} Q_{yc} \mathcal{L}_{\alpha q r \gamma}. \quad (\text{A } 13)$$

Finally, from (6.20)

$$\bar{\mathbf{M}}' = \text{const.} \times \int_{S_0} dS \int_{c_0} dc \langle \mathbf{Q} \rangle^4 * \mathcal{L} = \text{const.} \times \langle \mathbf{Q} \rangle^4 * \int_{S_0} dS \int_{c_0} dc \mathcal{L} = \langle \mathbf{Q} \rangle^4 * \bar{\mathbf{M}}. \quad (\text{A } 14)$$

Appendix B. Reversal symmetry of $\bar{\mathbf{M}}$

Following (A 3), we show that

$$(\mathbf{n} \times \mathbf{P} \times \mathbf{n})_{ijkl} = (\mathbf{n} \times \mathbf{P} \times \mathbf{n})_{lkji}. \quad (\text{B } 1)$$

Similar property for $\mathbf{n} \times \mathbf{C} \times \mathbf{n}$ is easily proven, implying the reversal symmetry of \mathcal{L}

$$\mathcal{L}_{ijkl} = \mathcal{L}_{lkji}. \quad (\text{B } 2)$$

Then, because the integration over directions in (6.22) is a linear operation, the reversal symmetry of $\bar{\mathbf{M}}$ (6.28) follows.

To prove (B 1), we first note that the major and minor symmetry of \mathbf{C} , and the symmetry of \mathcal{M}^{-1} , imply the major and minor symmetry of \mathcal{P} :

$$\mathcal{P}_{ijkl} = C_{ijpq} n_q \mathcal{M}_{pr}^{-1} n_s C_{srkl} = C_{klrs} n_s \mathcal{M}_{rp}^{-1} n_q C_{qpji} = \mathcal{P}_{klji} = \mathcal{P}_{jikl}. \quad (\text{B } 3)$$

Then

$$\begin{aligned} (\mathbf{n} \times \mathbf{P} \times \mathbf{n})_{ijkl} &= \epsilon_{ipq} n_p \mathcal{P}_{qjkr} n_s \epsilon_{rsl} = -\epsilon_{lsr} n_s \mathcal{P}_{krqj} n_p (-\epsilon_{qpi}) \\ &= \epsilon_{lsr} n_s \mathcal{P}_{rkij} n_p \epsilon_{qpi} = (\mathbf{n} \times \mathbf{P} \times \mathbf{n})_{lkji}. \end{aligned} \quad (\text{B } 4)$$

References

1. Ashby MF. 1970 The deformation of plastically non-homogeneous materials. *Phil. Mag.* **21**, 399–424. (doi:10.1080/14786437008238426)
2. Gurtin ME. 2002 A gradient theory of single-crystal viscoplasticity that accounts for geometrically necessary dislocations. *J. Mech. Phys. Solids* **50**, 5–32. (doi:10.1016/S0022-5096(01)00104-1)
3. Mindlin RD. 1964 Micro-structure in linear elasticity. *Arch. Ration. Mech. Anal.* **16**, 51–78. (doi:10.1007/BF00248490)
4. Eringen AC, Suhubi ES. 1964 Nonlinear theory of simple microelastic solids: I. *Int. J. Eng. Sci.* **2**, 189–203. (doi:10.1016/0020-7225(64)90004-7)
5. Cordero NM, Gaubert A, Forest S, Busso EP, Gallerneau F, Kruch S. 2010 Size effects in generalised continuum crystal plasticity for two-phase laminates. *J. Mech. Phys. Solids* **58**, 1963–1994. (doi:10.1016/j.jmps.2010.06.012)
6. Aslan O, Cordero NM, Gaubert A, Forest S. 2011 Micromorphic approach to single crystal plasticity and damage. *Int. J. Eng. Sci.* **49**, 1311–1325. (doi:10.1016/j.ijengsci.2011.03.008)
7. Arsenlis A, Parks DM, Becker R, Bulatov VV. 2004 On the evolution of crystallographic dislocation density in non-homogeneously deforming crystals. *J. Mech. Phys. Solids* **52**, 1213–1246. (doi:10.1016/j.jmps.2003.12.007)

8. Yefimov S, Groma I, van der Giessen E. 2004 A comparison of statistical-mechanics based plasticity model with discrete dislocation plasticity calculations. *J. Mech. Phys. Solids* **52**, 279–300. (doi:10.1016/S0022-5096(03)00094-2)
9. Groma I, Gyorgyi G, Kocsis B. 2007 Dynamics of coarse grained dislocation densities from an effective free energy. *Phil. Mag.* **87**, 1185–1199. (doi:10.1080/14786430600835813)
10. Nye JF. 1953 Some geometrical relations in dislocated crystals. *Acta Metall.* **1**, 153–162. (doi:10.1016/0001-6160(53)90054-6)
11. Kröner E. 1958 Kontinuumstheorie der Versetzungen und Eigenspannungen. *Ergeb. angew. Math.* 5. Berlin, Germany: Springer.
12. Kondo K. 1952 On the geometrical and physical foundations of the theory of yielding. *Proc. Jpn Natl Congr. Appl. Mech.* **2**, 41–47.
13. Cermelli P, Gurtin ME. 2002 Geometrically necessary dislocations in viscoplastic single crystals and bicrystals undergoing small deformations. *Int. J. Solids Struct.* **39**, 6281–6309. (doi:10.1016/S0020-7683(02)00491-2)
14. Arsenlis A, Parks DM. 1999 Crystallographic aspects of geometrically-necessary and statistically-stored dislocation density. *Acta Mater.* **47**, 1597–1611. (doi:10.1016/S1359-6454(99)00020-8)
15. Sun S, Adams BL, King W. 2000 Observations of lattice curvature near the interface of a deformed aluminum bicrystal. *Phil. Mag. A* **80**, 9–25. (doi:10.1080/01418610008212038)
16. El-Dasher BS, Adams BL, Rollett AD. 2003 Viewpoint: experimental recovery of geometrically necessary dislocation density in polycrystals. *Scr. Mater.* **48**, 141–145. (doi:10.1016/S1359-6462(02)00340-8)
17. Kysar JW, Saito Y, Oztop MS, Lee D, Huh WT. 2010 Experimental lower bounds on geometrically necessary dislocation density. *Int. J. Plast.* **26**, 1097–1123. (doi:10.1016/j.jiplas.2010.03.009)
18. Groma I, Gyorgyi G, Kocsis B. 2006 Debye screening of dislocations. *Phys. Rev. Lett.* **96**, 165503. (doi:10.1103/PhysRevLett.96.165503)
19. Mesarovic SDj, Baskaran R, Panchenko A. 2010 Thermodynamic coarse-graining of dislocation mechanics and the size-dependent continuum crystal plasticity. *J. Mech. Phys. Solids* **58**, 311–329. (doi:10.1016/j.jmps.2009.12.002)
20. Bertram A. 2012 *Elasticity and plasticity of large deformations—an introduction*, 3rd edn. Berlin, Germany: Springer.
21. Zheng QS, Spencer AJM. 1993 On the canonical representations for Kronecker powers of orthogonal tensors with application to material symmetry problems. *Int. J. Eng. Sci.* **31**, 617–635. (doi:10.1016/0020-7225(93)90054-X)
22. Eringen AC. 1999 *Microcontinuum field theory. I. Foundations and solids*. Berlin, Germany: Springer.
23. Eremeyev VA, Pietraszkiewicz W. 2012 Material symmetry group of the non-linear polar-elastic continuum. *Int. J. Solids Struct.* **49**, 1993–2005. (doi:10.1016/j.ijsolstr.2012.04.007)
24. Groma I. 1997 Link between the microscopic and mesoscopic length-scale description of the collective behaviour of dislocations. *Phys. Rev. B* **56**, 5807–5813. (doi:10.1103/PhysRevB.56.5807)
25. Mesarovic SDj. 2010 Plasticity of crystals and interfaces: From discrete dislocations to size-dependent continuum theory. *Theor. Appl. Mech.* **37**, 289–332. (doi:10.2298/TAM1004289M)
26. Hirth JP, Lothe J. 1992 *Theory of dislocations*. Reprint of the 2nd edn (1982). New York, NY: Wiley.
27. Mesarovic SDj. 2005 Energy, configurational forces and characteristic lengths associated with the continuum description of geometrically necessary dislocations. *Int. J. Plast.* **21**, 1855–1889. (doi:10.1016/j.jiplas.2004.09.002)
28. Yassar RS, Mesarovic SDj, Field DP. 2007 Micromechanics of hardening of elastic-plastic crystals with elastic inclusions. I—Dilute concentration. *Int. J. Plast.* **23**, 1901–1917. (doi:10.1016/j.jiplas.2007.03.013)
29. Kosevich AM. 1979 Crystal dislocations and the theory of elasticity. In *Dislocations in solids* (ed. FRN Nabarro), vol. 1, pp. 33–141. North-Holland Publishing Co.

30. Baskaran R, Akarapu S, Mesarovic SDj, Zbib HM. 2010 Energies and distributions of dislocations in stacked pile-ups. *Int. J. Solids Struct.* **47**, 1144–1153. (doi:10.1016/j.ijsolstr.2010.01.007)
31. Lothe J. 1982 Dislocations in anisotropic media. The interaction energy. *Phil. Mag. A* **46**, 177–180. (doi:10.1080/01418618208236217)
32. Bacon DJ, Barnett DM, Scattergood RO. 1979 Anisotropic continuum theory of lattice defects. *Prog. Mater. Sci.* **23**, 51–62. (doi:10.1016/0079-6425(80)90007-9)
33. Shu JY, Fleck NA, Van der Giessen E, Needleman A. 2001 Boundary layers in constrained plastic flow: comparison of non-local and discrete dislocation plasticity. *J. Mech. Phys. Solids* **49**, 1361–1395. (doi:10.1016/S0022-5096(00)00074-0)
34. Mesarovic SDj, Baskaran R. 2011 Interfaces in size-dependent crystal plasticity. In *Proc. 3rd Int. Conf. on Heterogeneous Material Mechanics (ICHMM-2011)*, 22–26 May, 2011, Shanghai.